Journal of Nano- and Electronic Physics
Vol. **17** No 6, 06020(5pp) (2025)

Журнал нано- та електронної фізики
Том **17** № 6, 06020(5cc) (2025)

OPEN ACCESS

REGULAR ARTICLE

Side Lobe Reduction Using Tapering and Windowing in Antenna Radiation Pattern for Radar Systems Applications

S. Santhanam[1,*], G. Thangavel[2,†], M.R. Khanna[3,‡], A.V. Shanthi[4,§], D. Murugesan[5,**], M. Alagarsamy[1,††]

[1] *Department of Electronics and Communication Engineering, K. Ramakrishnan College of Technology, Tiruchirappalli, Tamil Nadu, India*
[2] *Department of Electronics and Communication Engineering, University of Technology and Applied Sciences, Muscat, Sultanate of Oman*
[3] *Department of Information Technology, Vel Tech Multi Tech Dr. Rangarajan Dr. Sakunthala Engineering College, Avadi, Chennai, Tamil Nadu, India*
[4] *Department of Electronics and Communication Engineering, Prathyusha Engineering College, Tiruvallur – 602025, Tamil Nadu, India*
[5] *Department of Electronics and Communication Engineering, Kongunadu College of Engineering and Technology, Trichy - 621215, Tamil Nadu, India*

(Received 08 August 2025; revised manuscript received 12 December 2025; published online 19 December 2025)

An array of antennas is a radiating structure made up of components and radiators. Every radiator in this set has a unique induction field. Because of their close proximity, all of the components are within each other's induction fields. As a result, the radiation pattern they created would consist of the vector sum of each one separately. In systems like radar, communications via satellite, and medical imaging, where undesired sidelobe signals can impair target recognition or image quality, sidelobe minimization is essential. In this paper, the normalized radiation pattern of eight elements in a uniform linear array having uniform spacing between each element of $d = \lambda/2$ has been simulated along with sidelobe Level (SLL) reduction. The two methods studied are: Tapering using windowing by Hamming, Hanning, Blackman and Kaiser window with rectangular window as the reference. Array tapering using DFT with 20 numbers of elements, – 40 to 40 steering angle and Hamming window as the side-lobe control method. The array tapering and different windowing method has been studied with Hamming, Hanning Blackman and Kaiser window with rectangular window as reference. The gain pattern of 20 element array has been studied with – 40 to 40 steering angle and Hamming window as the side lobe control method. Radar systems, satellite communications, mobile communications networks, and the military and defense industries all use this SLL technology.

Keywords: Array antenna, Far field pattern, Window method, Array tapering, Side lobe level, Radar applications.

DOI: 10.21272/jnep.17(6).06020 PACS numbers: 61.05.cp, 61.82.Fk, 73.43.Qt

1. INTRODUCTION

Numerous applications and utilities, which include mobile phones, communications through satellites, radar, sonar, and even more recent wireless internet connections like the Internet of Things (IoT) in addition to medical networks, have made wireless networking and communication indispensable to our daily lives [1]. which uses beam-forming and antenna arrays to increase the power of the necessary signals while decreasing unwanted interfering signals. The goal is to increase the system's ability, reliability of service, along with information rates. The optimized algorithm [2] and 12-element time-modulated asymmetric elliptical antenna array [3] have been used to generate the radiation pattern of non-uniform series-fed microstrip patch antennas.2D arrays are currently widely used in MIMO as well as 5G systems to handle multiple broadcast or arriving signals [4].

* Correspondence e-mail: suganthis.ece@krct.ac.in
† gunasekaran.thangavel@utas.edu.om
‡ rajeshkhanna@veltechmultitech.org
§ shanthivijaygm@gmail.com
** dlingam6@gmail.com
†† manjunathankrct@gmail.com

Cite this article as: S. Santhanam et al., *J. Nano- Electron. Phys.* 17 No 6, 06020 (2025) https://doi.org/10.21272/jnep.17(6).06020

Consequently, it is advised that the antennas in the array reduce emission toward other directions, particularly at the side-lobes, while forming the main-lobe toward the intended signal direction. An antenna for the low sidelobe level (SLL) slot array [5] is designed using a W-band uneven power divider. Significantly raising the flare angle can reduce antenna clutter, reducing the length of the antenna can increase its bandwidth, and short antennas are advantageous for targets close to the surface [6]. High data rate communication and millimeter-wave radar benefit from antennas with radiation efficiency greater than 90% [7], good side lobe size for cost-effective 60 GHz applications [8], and antennas with an efficiency of roughly 97% are ideal for satellite communication systems and radar [9]. Front-to-back ratios for radar applications need to be better than 10.7 dB [10], and shoulder-shaped antennas [11] with flat emission patterns were made for 77 GHz automotive radar application in [12].

Reducing side lobe level is one of the elements in radar systems that enhance array antenna performance. The array antenna's antenna elements must have distinct weighting factors in order to produce beam patterns that are below side lobe level. In order to get varied weight factors, the sides are lowered in extent using unequal power dividers [13]. It is anticipated that the next 5th-generation (5G) antenna systems will use a single multi-beam array using spaced division multiple access (SDMA) to serve numerous users concurrently in the same frequency range [14]. Suppressing inter-user interference is essential for improved communication quality and capacity since interference, not noise, dominates such systems [15]. In this paper, we have analyzed the linear array antenna gain pattern with tapering techniques.

2. DESIGN EQUATION-LINEAR ARRAY ANTENNA

Narrow directional beams produced by arrays of antennas can be electrically or physically directed in various directions. Adjusting each phase of the electrical current which feeds the array elements allows for electrical steering. Arrays with beams that may electrically steer them are known as phased arrays. In most cases, the array's array ratio provides a complete description of it. The array factor allows the designer to determine the arrays' (1) 3-dB beamwidth; (2) null-to-null beamwidth; (3) the distance that is determined between the initial sidelobe in addition the dominant peak; (4) the height that represents the initial sidelobe in relation from the main beam; (5) the nulls' location; (6) the sidelobe's rate of reduce; and (7) the grating lobes' destinations. A linear array antenna with identical elements is depicted in Fig. 1. In (a), d, and this is frequently stated in frequency units, indicates a component separation. Assume that an array's phase indicator is element 1. Given that $K = 2\Pi/\lambda$, the arrangement of elements makes it evident that each outgoing waves which achieves the nth component enters its phase within the $(n+1)^{th}$ element prior $Kd\sin\psi$.

The averaged phase is unaffected by φ distance from nearest observed point P. Considering isotropic components, an electrical field at a far field observation position having direction-sine identical to $\sin\psi$ is

$$E(\sin\psi) = \sum_{i=1}^{N} e^{j(i-1)(kd\sin\psi)} \tag{1}$$

Highest value of $|E(\sin\psi)|$ is equivalent to $\psi = 0$ and occurs at $|E\sin\psi|$. The structure of standardized intensity [10] is therefore equal to

$$|E_n(\sin\psi)| = \frac{1}{N}\left|\frac{\sin((Nkd\sin\psi)/2)}{\sin((kd\sin\psi)/2)}\right| \tag{2}$$

The standardized bilateral array scheme, often known as the radiation electromagnetic pattern, is supplied by

$$|G(\sin\psi)| = \frac{1}{N^2}\left(\frac{\sin((Nkd\sin\psi)/2)}{\sin((kd\sin\psi)/2)}\right)^2 \tag{3}$$

For N = 8, Fig. 1(b) plots Eq. (4) against sinθ. Anisotropic to the azimuth angle ($\sin\psi = 0$), the radiated G($\sin\psi$) waveform is cylindrical symmetrical along its center. As a result, its values throughout the range decide it entirely ($0 < \psi < \Pi$). In order to steer the primary ray of an array into the direction-sine $\sin\psi_o$, any two neighbouring elements must have a phase difference of kd $\sin\psi_o$. Adjusting the direction in which the present force is supplied to each array element allows for electronic completion of this task.

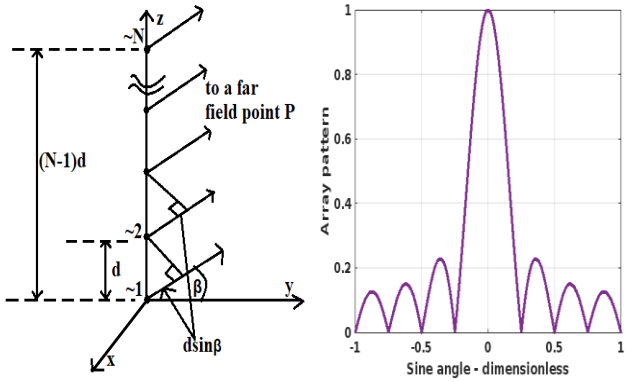

(a) (b)

Fig. 1 – (a) Eight elements in a uniform linear array having uniform spacing between each element of $d = \lambda/2$ (b) Normalized radiation pattern

The standardized patterns of radiation for this instance may be expressed as

$$\left|G(\sin\beta)\right| = \frac{1}{N^2}\left(\frac{\sin[(Nkd/2)(\sin\beta-\sin\beta_0)]}{\sin[(kd/2)(\sin\beta-\sin\beta_0)]}\right)^2 \qquad (4)$$

3. ARRAY TAPERING

However, the first side lobe, 13.46 dB below the main lobe, may not be sufficient for most radar functions. The array must be designed to reduce the side-lobe levels by emitting much less power at the periphery and more in the core. The compromise among side-lobe lowering as well as primary beam broadening must be considered when selecting a tapering procedure for a particular radar operation.

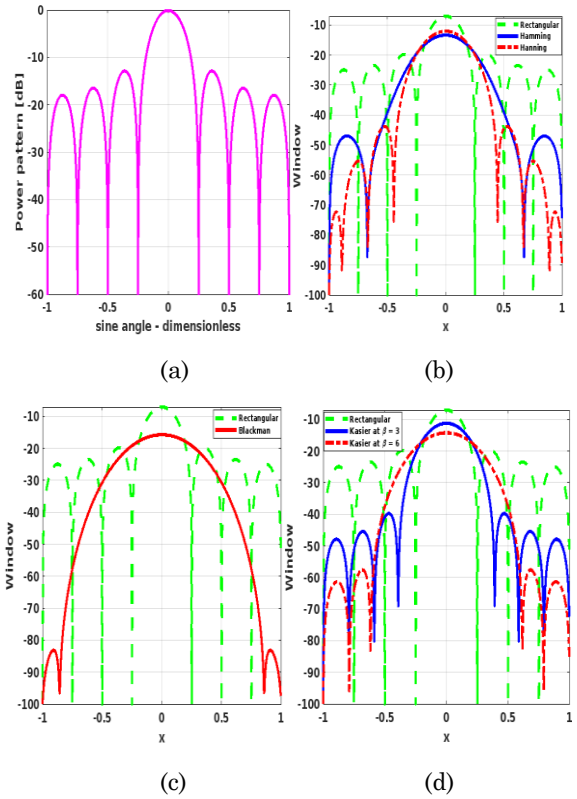

Fig. 2 – (a) $N = 8$ & $d = \lambda/2$ normalized radiation plot. Comparison of windowing function with Rectangular as reference (b) Hamming & Hanning (c) Blackman (d) Kaiser with $\beta = 3$ & 6

Fig. 2(b) to (d) illustrates the effects of most of the popular windows on the array's patterns in terms of peak reductions together with primary beam broadening, using the rectangular windows to serve as baseline. The linear array's radiation power pattern with a rectangular window is displayed in Fig. 2(a). In contrast to rectangular and Hamming windows, the side-lobe level has decreased in these arrays using Hamming and Blackman windows, as illustrated in Figs. 2(b) and (c). As seen in Fig. 2(d), the side-lobe value has decreased as the Kaiser window's β value has increased in comparison to the reference window.

4. ARRAY TAPERING USING DFT

The linear array about size N, component separation d, and length L is seen in Fig. 3.

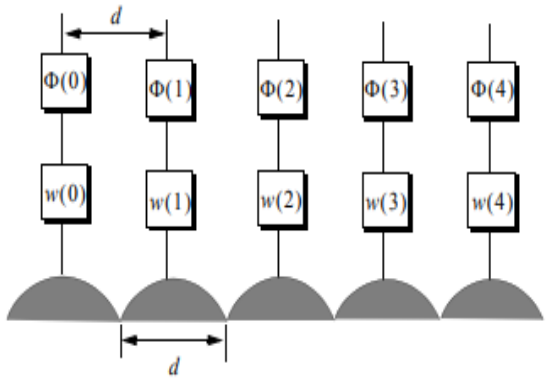

Fig. 3 – Linear array of dimension 5, featuring hardware for phase shifting and tapering

The radiators are d-diameter circular dishes. Let $w(n)$ and $\Phi(n)$ stand for the tapering as well as phase shifting sequences, respectively. At a distant field point, the standardized electric field according to direction-sine $\sin\psi$ using a window sequence's symmetry attribute is

$$E(\sin\psi) = e^{j\phi_0}\left[w(0)+w(1)V_1^1+.....+w(N-1)V_1^{N-1}\right]$$
$$= e^{j\phi_0}\sum_{n=0}^{N-1} w(n)V_1^n \qquad (5)$$

The definition of the sequence's w(n) discrete Fourier transform is

$$W(q) = \sum_{n=0}^{N-1} w(n)e^{-\frac{(j2\pi nq)}{N}} \;;\; q = 0,1,.....,N-1 \qquad (6)$$

The set $\{\sin\psi_q\}$ that equals the DFT kernel for V_1 is

$$\sin\psi_q = \frac{\lambda q}{Nd} \;;\; q = 0,1,....,N-1 \qquad (7)$$

By combining the above two equs., we get

$$E(\sin\psi) = e^{j\phi_0}\,W(q) \qquad (8)$$

The modulus of the aforementioned equation is used to calculate the unidirectional array pattern. Consequently, a tapering linear array with circular dishes' uniline radiation pattern is

$$G(\sin\psi) = G_e\left|W(q)\right| \qquad (9)$$

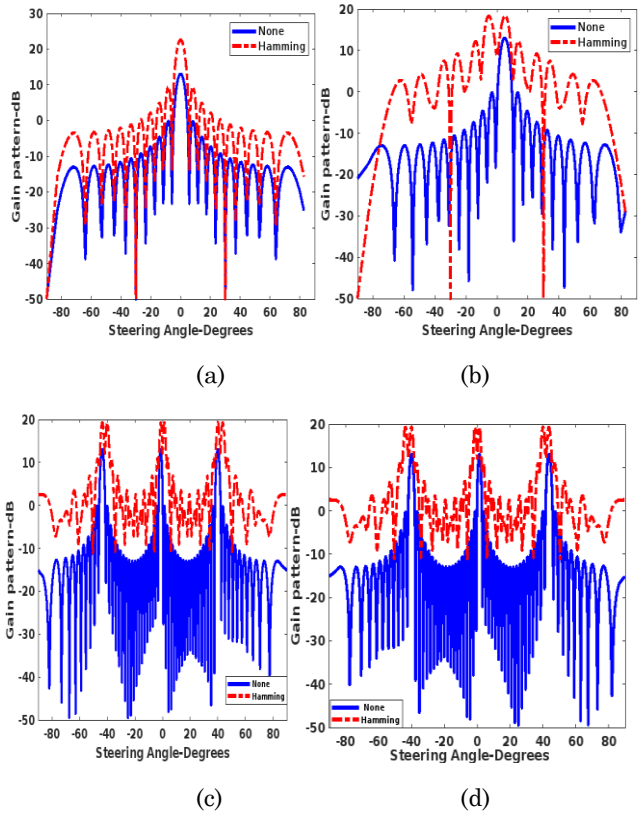

Fig. 4 – Comparison of windowing effect in array gain pattern using DFT with $N = 20$ &. (a) Element spacing = 0.5 & Steering angle = 0° (b) Element spacing = 0.5 & Steering angle = 5° (c) Element spacing = 1.5 & Steering angle = 40° (d) Element spacing = 1.5 & Steering angle = – 40°

Where the element pattern is denoted by G_e. A small number of bits from the Transmit/Receive (TR) modules are frequently used in practice to create phase shifters. The difference between the desired and real quantized phases, or quantization error, consequently affects the side-lobe levels.

Table 1 – Input description of radiation pattern Simulation-Linear array

Description	Value	Description	Value
Number of elements in array	20	Element spacing in lambda units	0.5 & 1.5
Window for side-lobe control	Hamming	Steering angle (degree)	0,5,40 & – 40
If no weighting During side-lobe control, apply weighting as specified in the window	– 1 1	Perfect quantization Use 2^{nbits} quantization levels	Negative Positive

As a measure of the true sine-space (sine wave the steering angle), Fig. 4 displays the linear arrays gain patterns using the input list from Table 1. Beamwidth, bandwidth, and convergence speed must all be taken into account while evaluating the many methods that various writers have suggested employing optimal algorithms. The basic MATLAB code for tapering and windowing approaches from SLL reduction was proposed in this study.

5. CONCLUSION

The fundamentals of radar antenna radiation pattern as well as mathematical deductions pertaining to power gain—the crucial variable in radar equations have been examined. After analyzing the electric field strength in the far field region geometry, it was found that both the antenna's size and operating wavelength affect the distant field. The radiation patterns of two types of antennas are computed and simulated. The circular dish reflectors, which are commonly utilized in radar and microwave applications due to their easy construction and design, have closed form far field expressions. Additionally, the impact of AI, machine learning, along with advanced materials will drive the integration of SLL technology with 5G and 6G.

REFERENCES

1. K. Pałczynski, S ´Smigiel, M. Gackowska, D. Ledzinski, S. Bujnowski, Z. Lutowski, *Sensors* **21**, 8025 (2021).
2. H. Khalili, K. Mohammadpour-Aghdam, S. Alamdar, *International Journal of Electronics and Communications* **176**, 155143 (2024).
3. S. Kumar, G. Ram, D. Mandal, R. Kar, *IEEE Space, Aerospace and Defence Conference (SPACE)*, Bangalore, India, 1196 (2024).
4. D.G. Riviello, F. Di Stasio, R. Tuninato, *Electronics* **11**, 330 (2022).
5. L. Li, H. Gao, B. Zhang, C. Jin, *Int.J.of Antennas & propagation*, 7226780, 1 (2024).
6. D. Uduwawala, M. Norgren, P. Fuks, A.W. Gunawardena, *IEEE Transactions on Geoscience and Remote Sensing* **42** No 4, 732 (2004).
7. R.A. Alhalabi, G.M. Rebeiz, *IEEE Transactions on Antennas and Propagation* **57** No 11, 3672 (2009).
8. X. Chen, K. Wu, L. Han, F. He, *IEEE Transactions on Antennas and Propagation* **58** No 6, 2126 (2010).
9. A.M. Barani, R. Latha, R. Manikandan, *International Journal of Recent Technology and Engineering* **08** No 4S5, 134 (2019).
10. A.K. Tripathi, B.K. Singh, *International Conference on Microwave and Photonics*, Dhanbad, 1 (2013).
11. O.K. Eyiogwu, *IntechOpen*, Dec. 21, (2022)..
12. S. Santhanam, S. Govindasamy, M. Thilagaraj, R. Radhakrishnan, T.S. Palavesam, M. Alagarsamy, *International Journal on Communications Antenna and Propagation* **13** No 4, 213 (2023).
13. B.R. Mahafza, *Radar Systems Analysis and Design Using MATLAB*, 4th edition, deciBEL Research, (Inc.Chapman & Hall/CRC, 2022).
14. S.J. Park, D.H. Shin, S.O. Park, *IEEE Transactions on Antennas and Propagation* **64** No 3, 923 (2016).
15. Y. Aslan, S. Salman, J. Puskely, A. Roederer, A. Yarovoy, *Proc. 13th Eur.Conf. Antennas Propag.*, Krakow, Poland, (2019).

Зменшення бічних пелюсток за допомогою звуження та віконування в діаграмі спрямованості антени для радіолокаційних систем

S. Santhanam[1], G. Thangavel[2], M.R. Khanna[3], A.V. Shanthi[4], D. Murugesan[5], M. Alagarsamy[1]

[1] *Department of Electronics and Communication Engineering, K. Ramakrishnan College of Technology, Tiruchirappalli, Tamil Nadu, India*
[2] *Department of Electronics and Communication Engineering, University of Technology and Applied Sciences, Muscat, Sultanate of Oman*
[3] *Department of Information Technology, Vel Tech Multi Tech Dr. Rangarajan Dr. Sakunthala Engineering College, Avadi, Chennai, Tamil Nadu, India*
[4] *Department of Electronics and Communication Engineering, Prathyusha Engineering College, Tiruvallur – 602025, Tamil Nadu, India*
[5] *Department of Electronics and Communication Engineering, Kongunadu College of Engineering and Technology, Trichy – 621215, Tamil Nadu, India*

Антенна решітчаста антена – це випромінювальна структура, що складається з компонентів та випромінювачів. Кожен випромінювач у цьому наборі має унікальне індукційне поле. Через їх близьке розташування всі компоненти знаходяться в межах індукційних полів один одного. Як результат, діаграма спрямованості, яку вони створюють, складатиметься з векторної суми кожного з них окремо. У таких системах, як радар, супутниковий зв'язок та медична візуалізація, де небажані сигнали бічних пелюсток можуть погіршити розпізнавання цілі або якість зображення, мінімізація бічних пелюсток є важливою. У цій статті було змодельовано нормалізовану діаграму спрямованості восьми елементів в рівномірній лінійній решітці з рівномірною відстанню між кожним елементом $d = \lambda/2$ разом зі зниженням рівня бічних пелюсток (SLL). Досліджено два методи: звуження з використанням віконування за допомогою вікна Хеммінга, Хеннінга, Блекмана та Кайзера з прямокутним вікном як опорним. Звуження решітчастої решітчастої антени з використанням DFT з 20 кількістю елементів, кутом повороту від –40 до 40 та вікном Хеммінга як методом керування бічними пелюстками. Звуження решітки та різні методи віконування досліджувалися з використанням вікна Хеммінга, Хеннінга, Блекмана та Кайзера з прямокутним вікном як еталоном. Діаграма посилення 20-елементної решітки досліджувалася з кутом повороту напрямку від – 40 до 40 та вікном Хеммінга як методом керування бічними пелюстками. Радіолокаційні системи, супутниковий зв'язок, мережі мобільного зв'язку, а також військова та оборонна промисловість використовують цю технологію SLL.

Ключові слова: Антенна решітка, Діаграма спрямованості дальнього поля, Метод вікна, Звуження решітки, Рівень бічних пелюсток, Застосування в радіолокації.